Material behavior during reflood test QUENCH-12 with a VVER bundle. Results of ISTC project # 1648.2

presented by J. Stuckert

VVER Materials Meeting

Institute of Apllied Materials

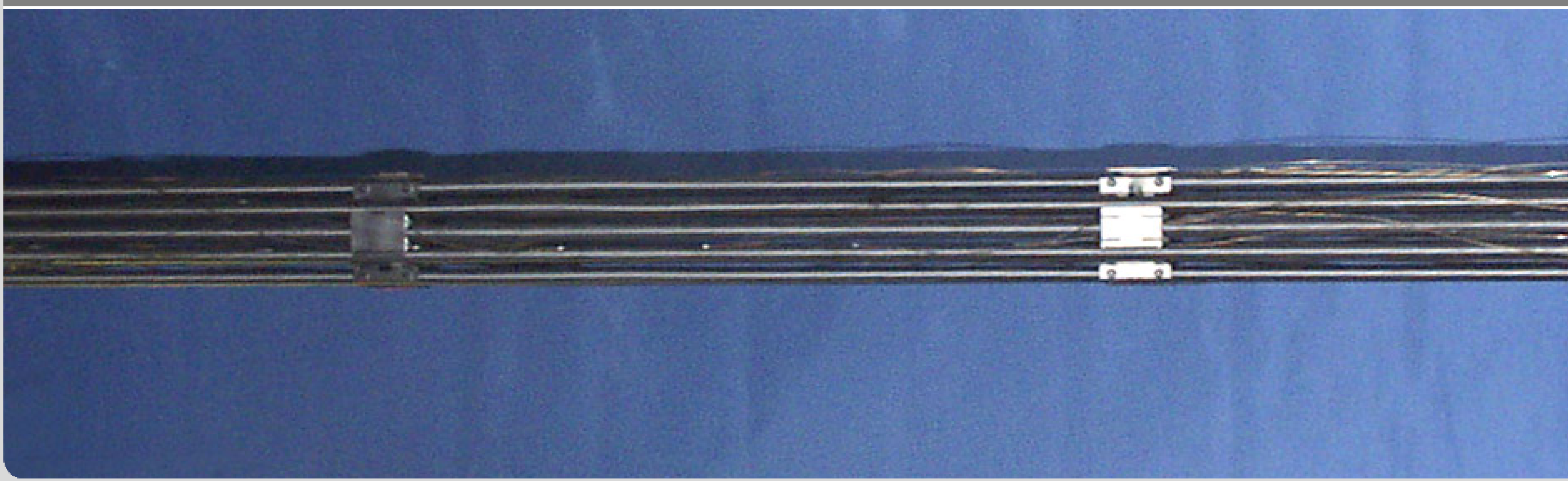

Objectives of the QUENCH-16 test

- investigation of the effects of VVER materials and bundle geometry on core reflood

- comparison with the PWR bundle on the base of repeat of the test QUENCH-06 (ISP-45) scenario

Comparison of PWR and VVER test columns

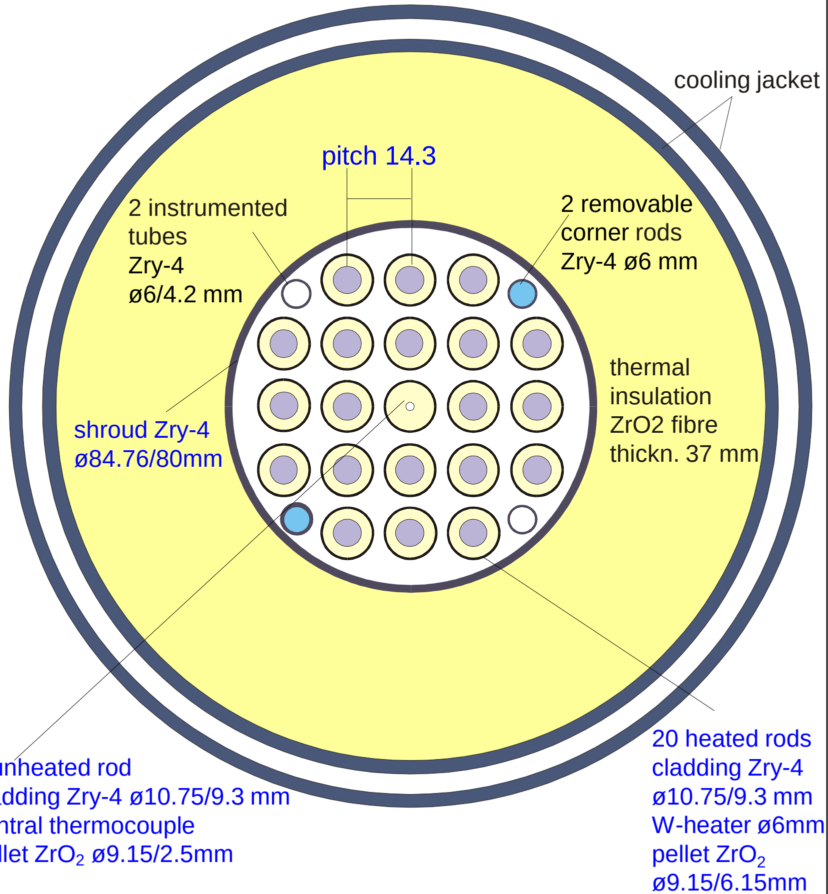

Cross section of the PWR test column

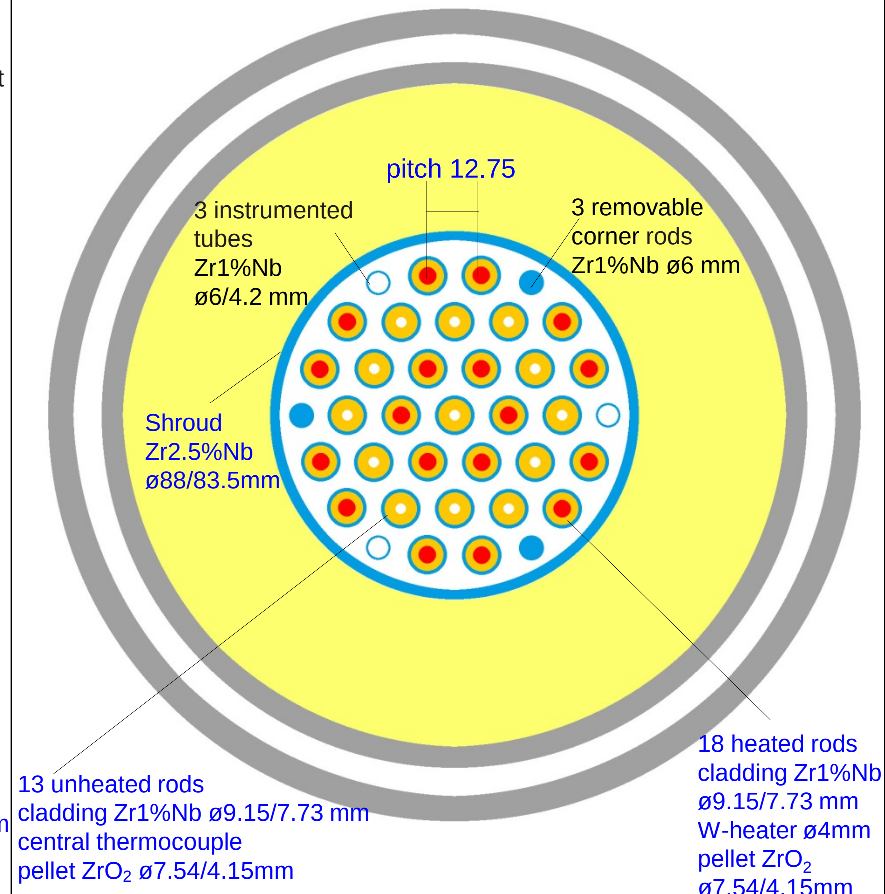

Cross section of the VVER test column (QUENCH-12)

Time schedule of Project performance

July 1999	**1st Proposal from RIAR and ELECTROSTAL on a VVER bundle test in the QUENCH facility**
2001	**ISTC development grant for Project 1648**
October 2002	**Recommendation of 2nd CEG-CM (Karlsruhe) for 1648.2 with highly priority**
March 2003	**Approval of Project 1648.2 by the ISTC Governing Board**
June 2004	**Start of Project 1648.2**
March 2005	**Contract between RIAR and KIT on delivery of the VVER bundle components**
October 2005	**Delivery of bundle components to KIT:** *1) etched and anodized Zr1%Nb cladding tubes, 2)Zr2.5%Nb shroud tube, 3) Zr2.5%Nb flange tube, 4) Zr1%Nb holder rods, 5)Zr1%Nb corner rods, 6) Zr1%Nb corner tubes, 7) Zr1%Nb spacing grids.*
27 September 2006	**Conducting of the QUENCH/VVER test (QUENCH-12) by KIT**
2006 - 2008	**Evaluation of the test data; metallographic examination of bundle by RIAR and KIT**
December 2007	**Report FZKA-7353 on the post-test modelling with the SVECHA code (IBRAE-KIT-ITU)**
March 2008	**Report FZKA-7307on results of the QUENCH-12 test**

Test bundle preparation

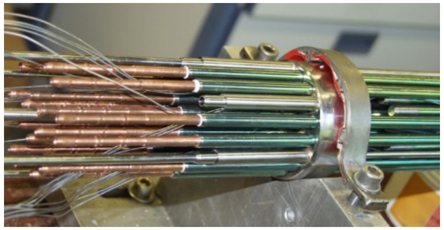

bundle bottom

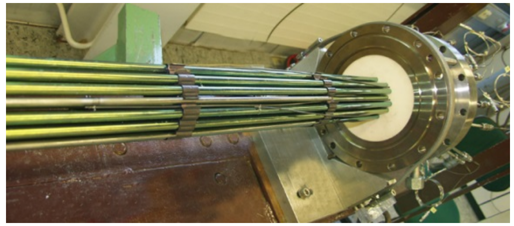

bundle top

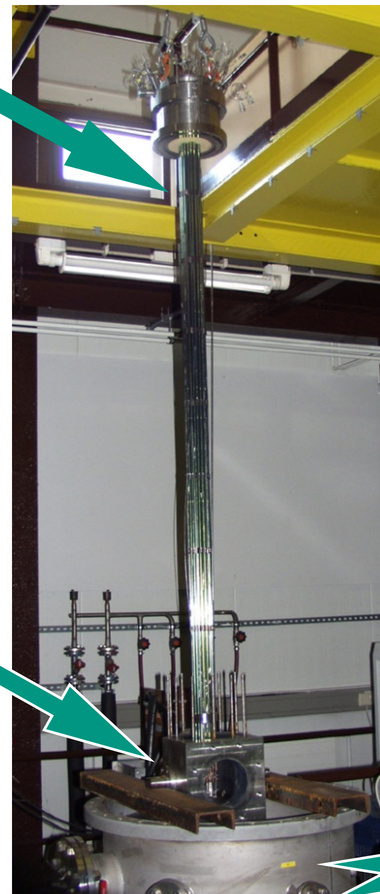

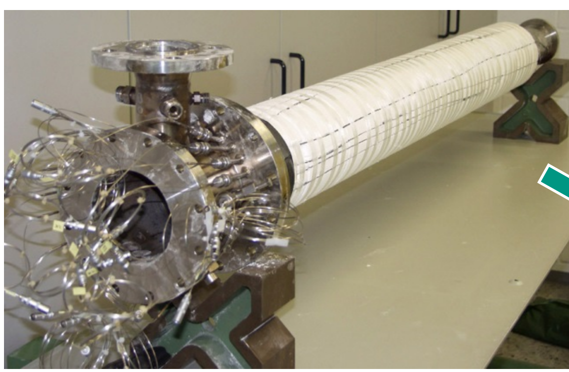

shroud with heat insulation

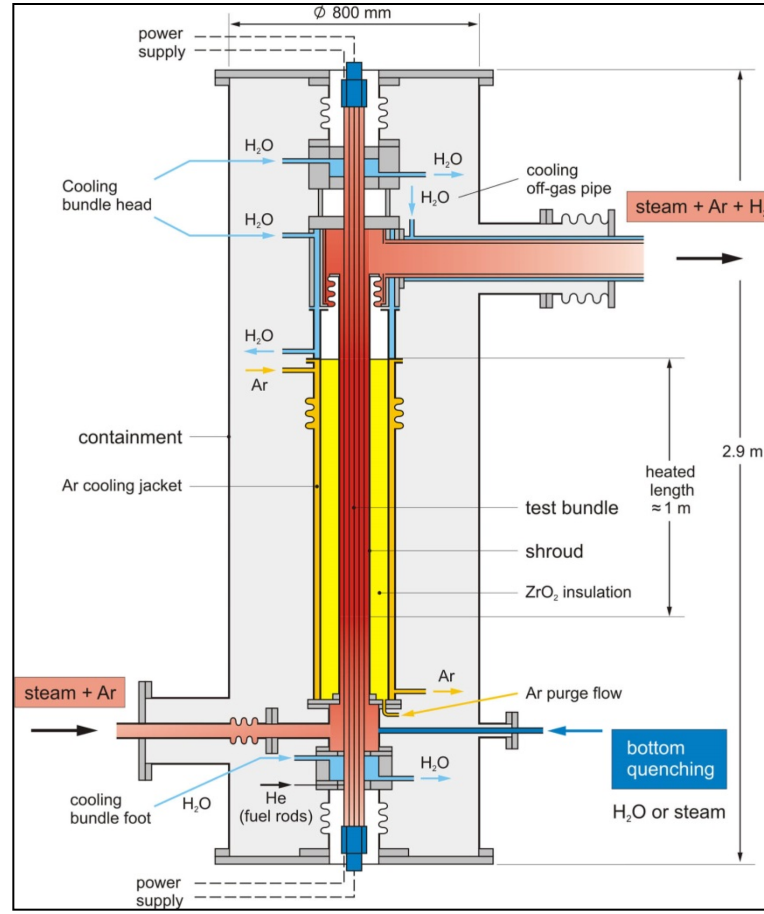

test containment with instrumented bundle

Pre-test modelling support:

1. SCDAP/SIM simulations: *Paul Scherer Institute, Switzerland*.

2. ICARE/CATHARE simulations: *Kurchatov Institute, Moscow, with support from IRSN Cadarache*).

Test performance: el. power profile in accordance to the pre-test calculations provided good reproduction of temperature history in comparison with the reference test QUENCH-06

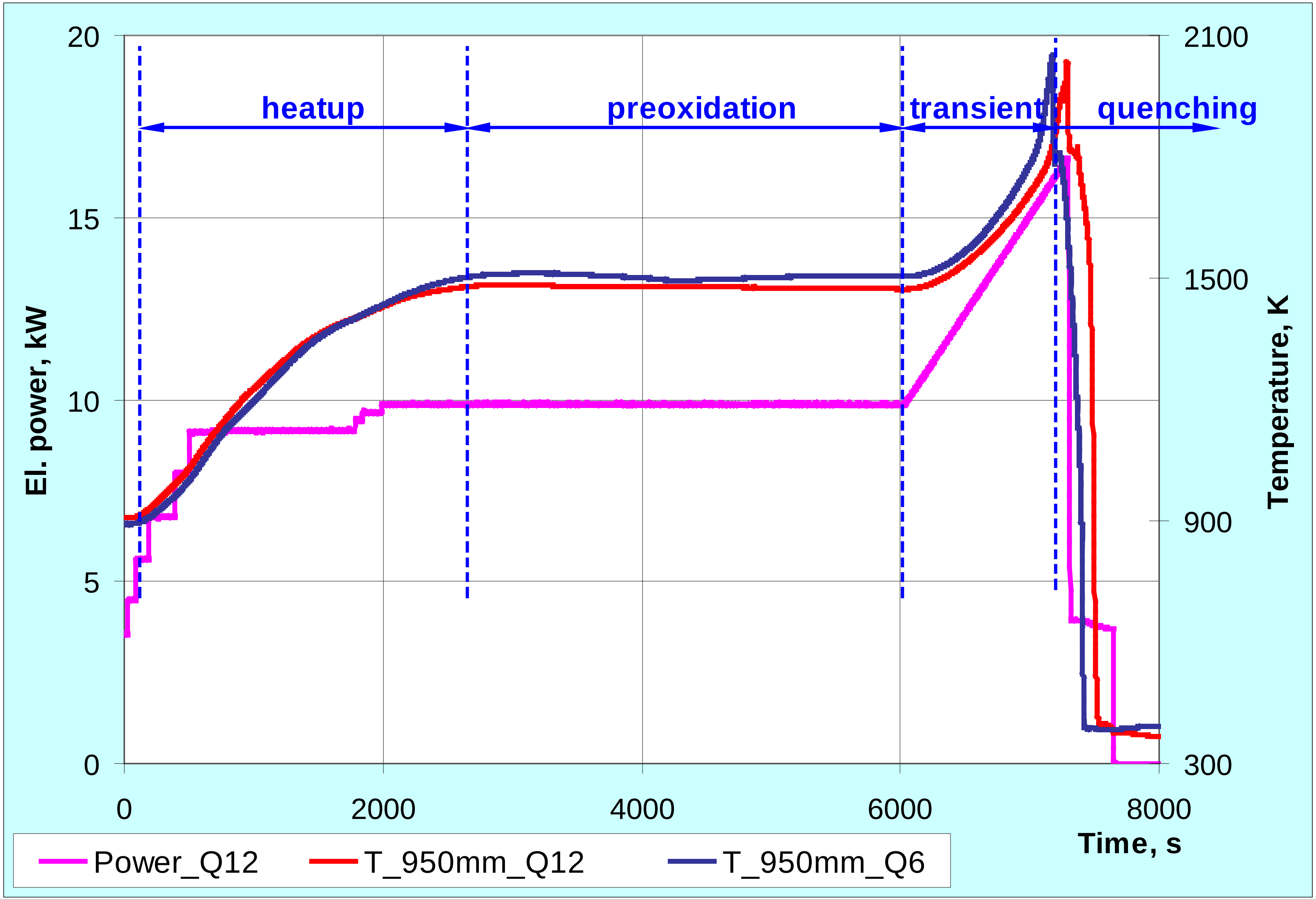

QUENCH-12: inhomogeneous radial temperature distribution

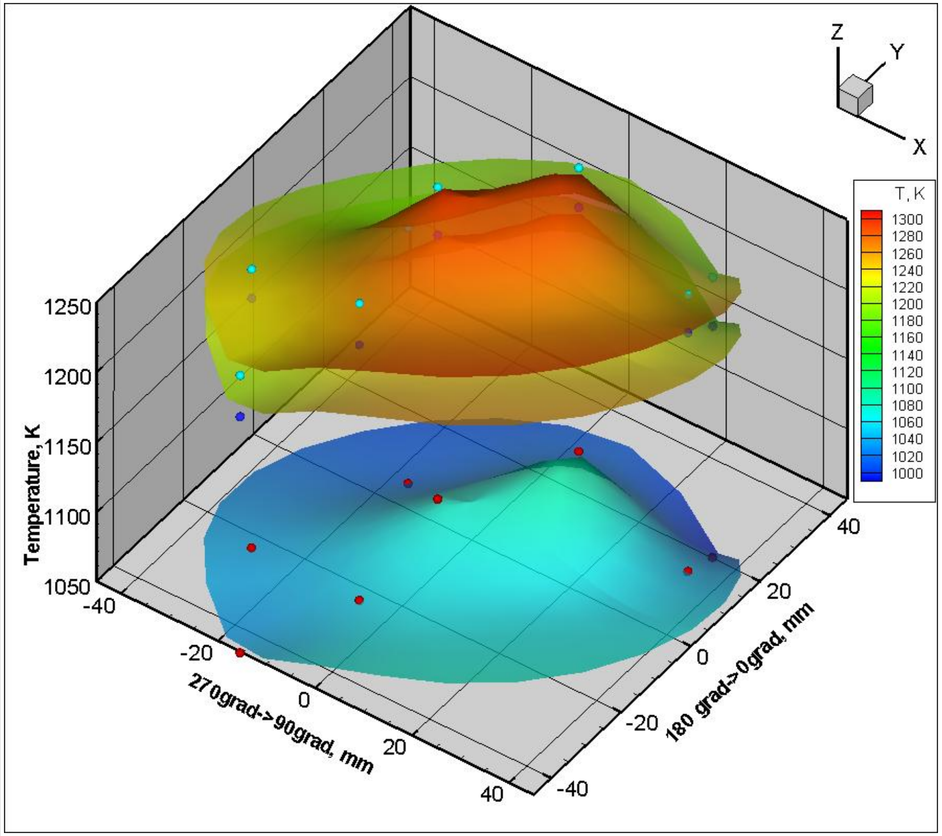

550 mm

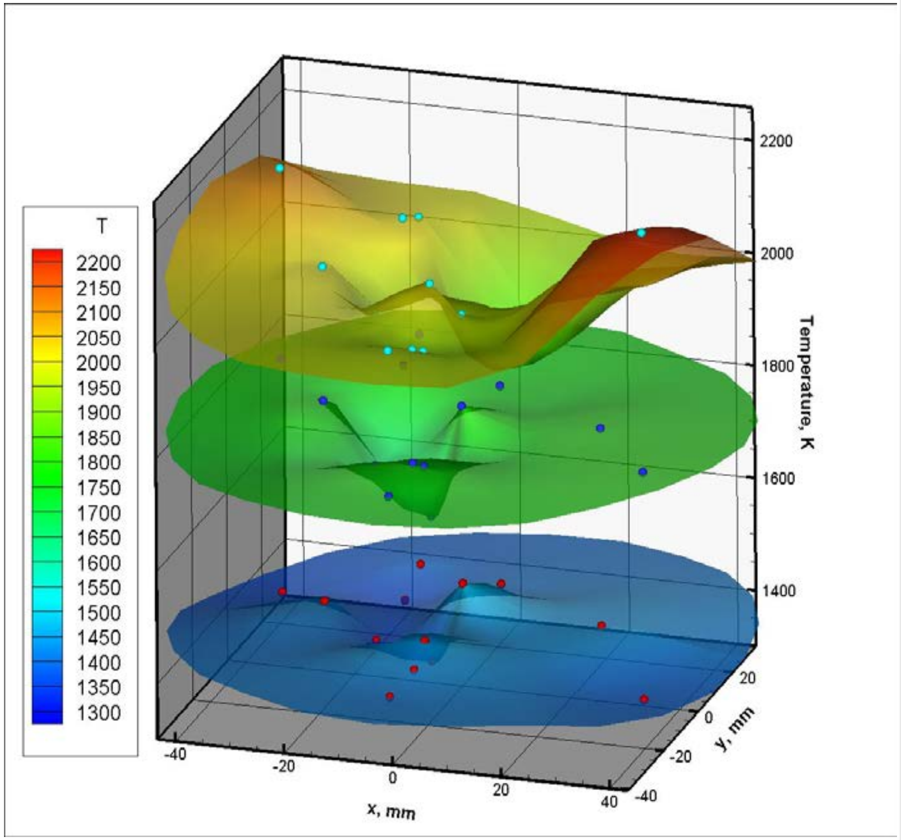

950 mm

temperature distributions for three time points (from bottom to top):
1) 5960 s (end of pre-oxidation), 2) 7150 s (middle of transient), 3) 7265 s (before reflood)

Axial bundle temperature profiles for QUENCH-06 and QUENCH-12 on beginning and end of transient phase

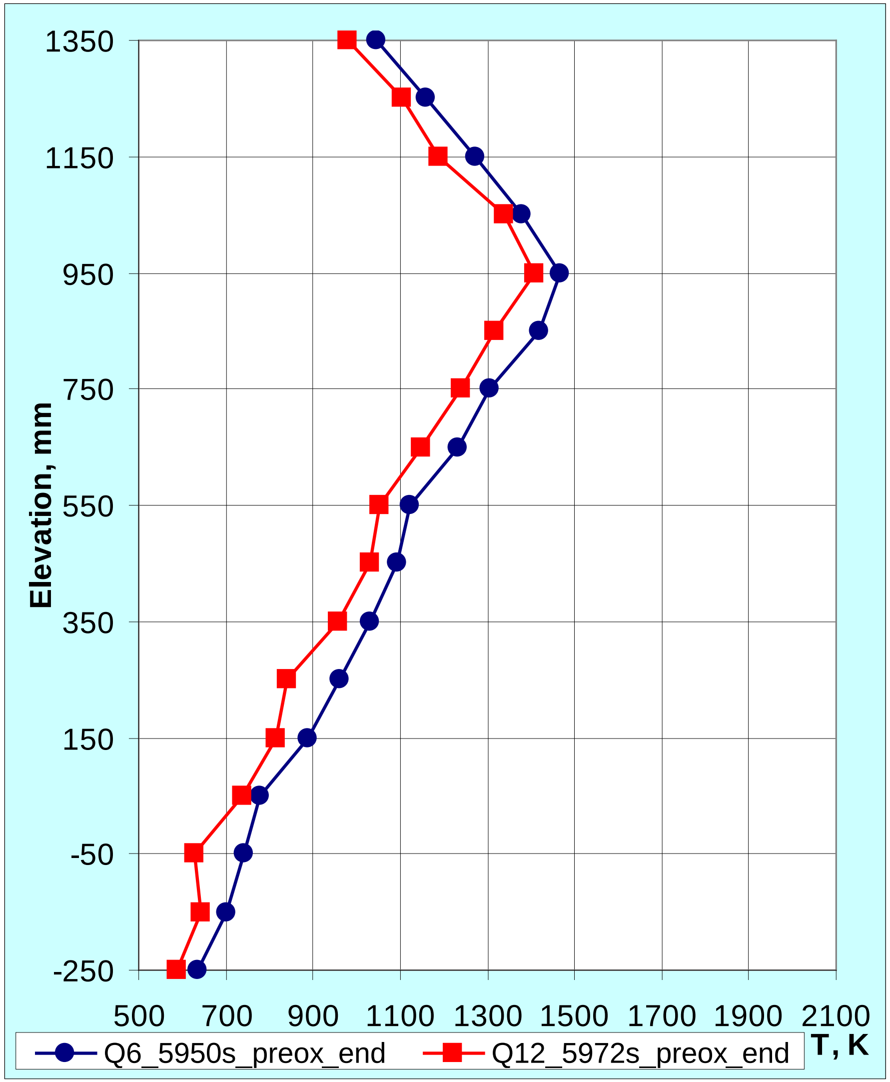

beginning of transient

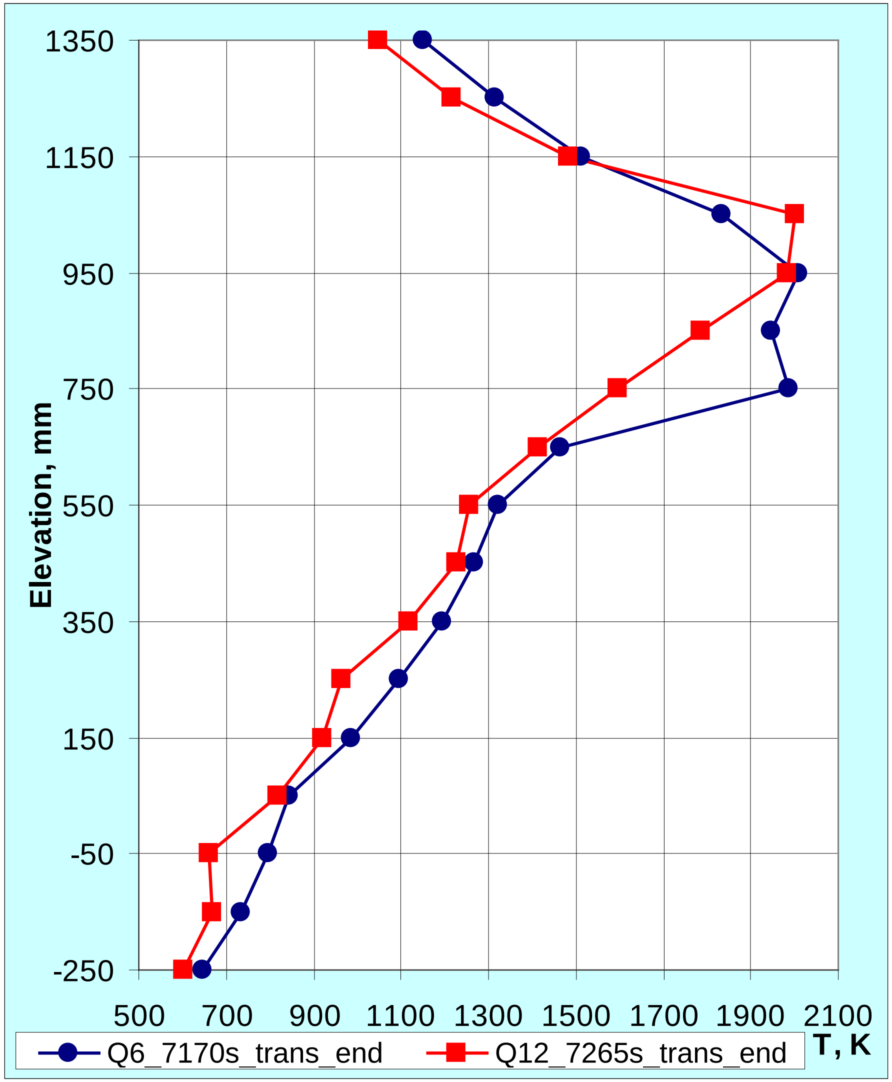

end of transient

Comparison of hydrogen release during QUENCH-12 and QUENCH-06

Karlsruhe Institute of Technology

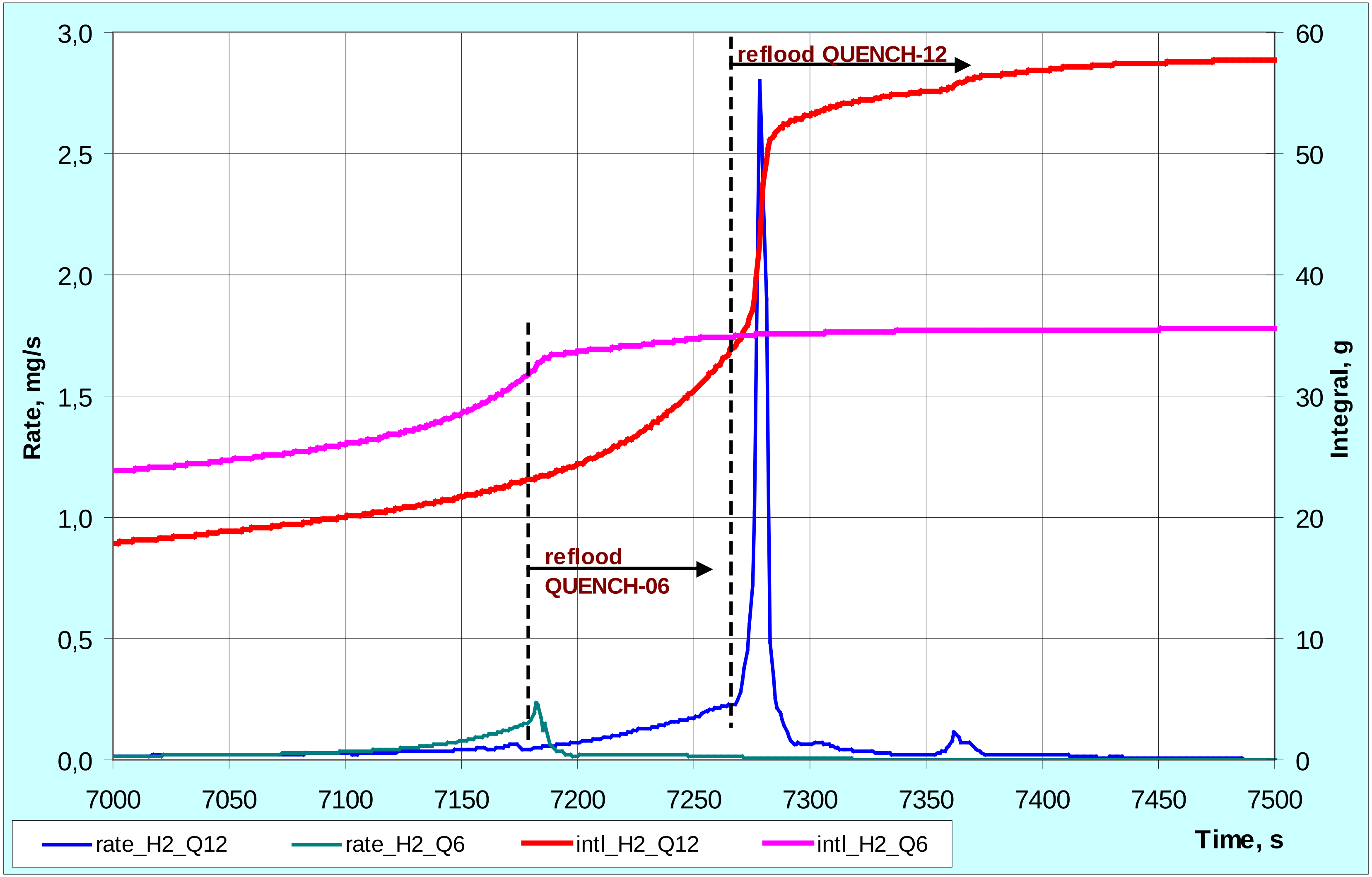

Comparison of hydrogen uptake by bundle during QUENCH-06 and QUENCH-12

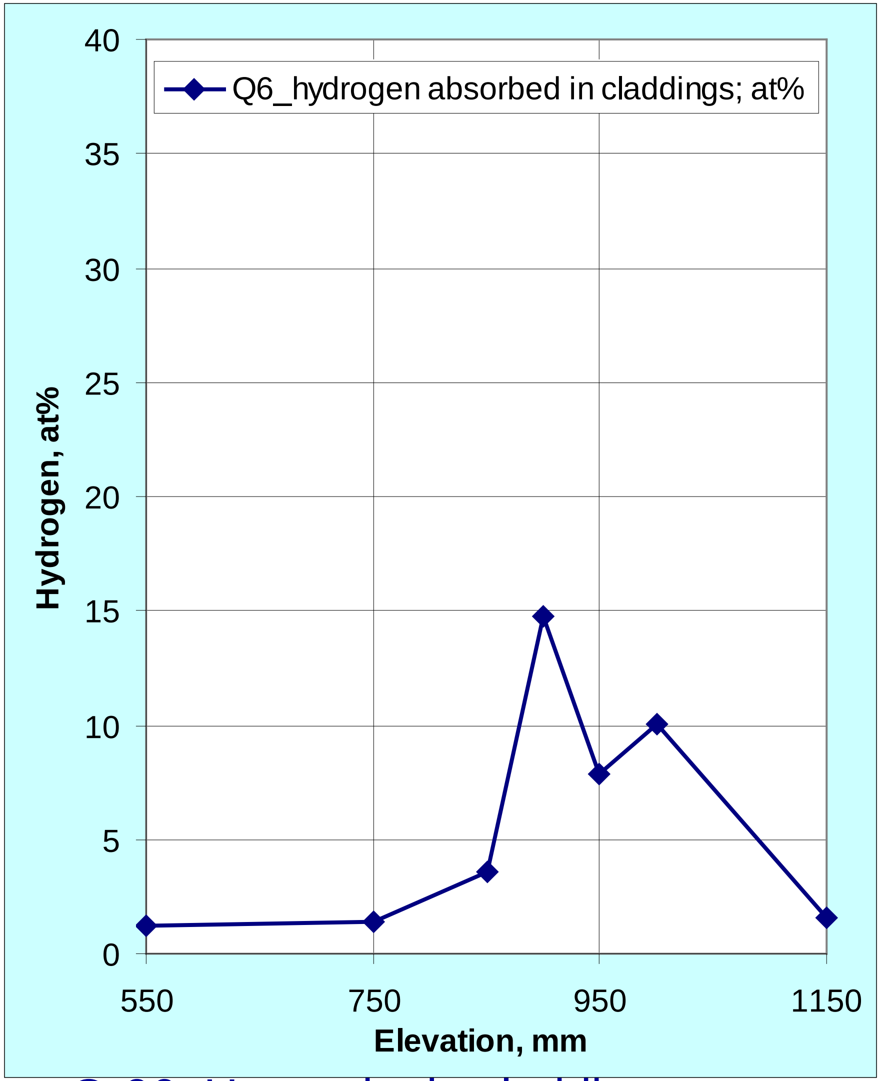

Q-06: H_2 uptake in cladding measured by hot extraction

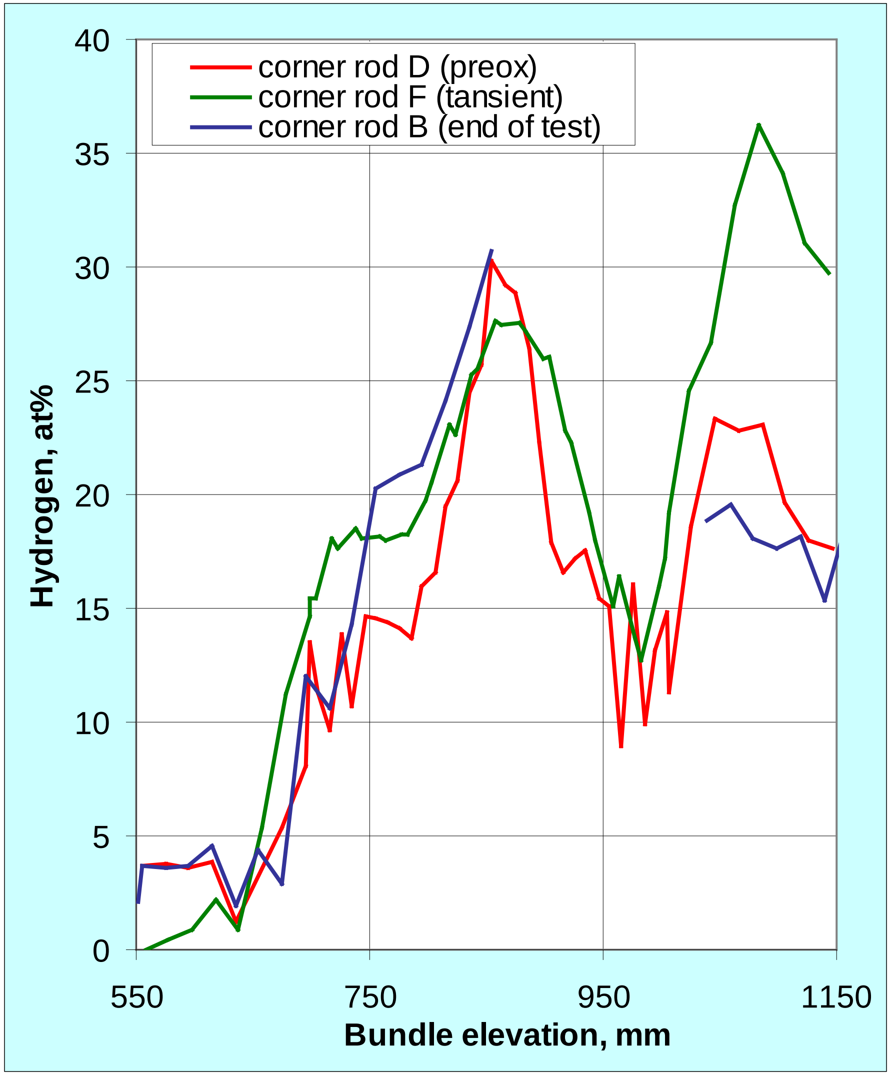

Q-12: H_2 uptake in corner rods measured by neutron radiography

QUENCH-12: axial sections of different ZrO_2 spalling intensity on corner rods withdrawn during the test

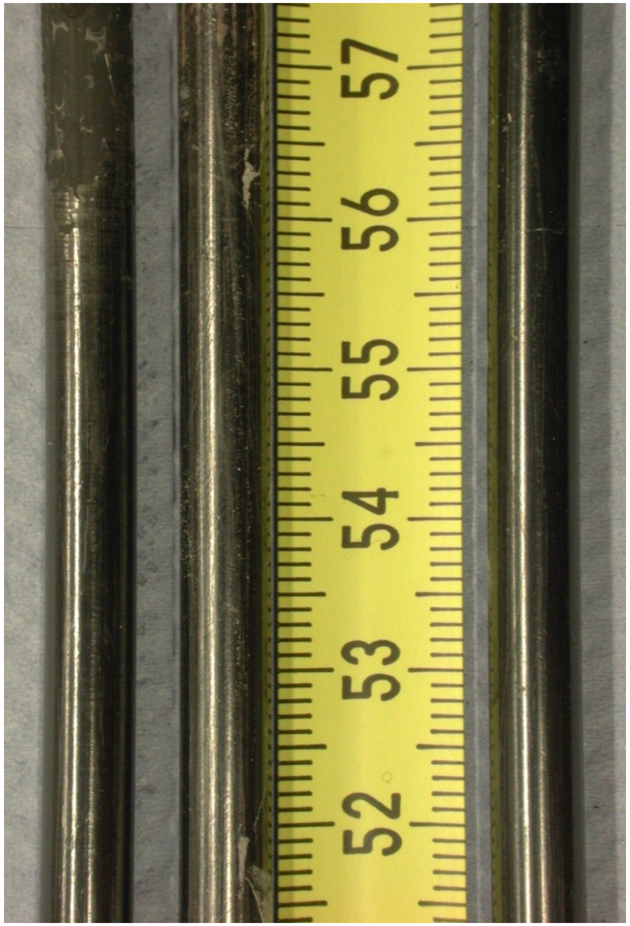

B after test | F before reflood | D after preoxidation

F | D

F | D

QUENCH-12: Structure of the residual oxide layer on the surface of three withdrawn corner rods at different bundle elevations

1st rod 700 mm	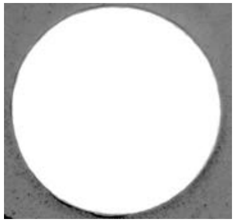	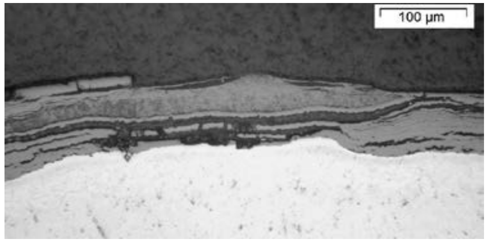	2nd rod 940 mm	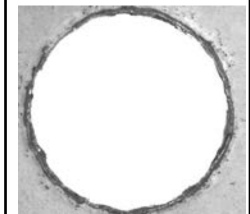	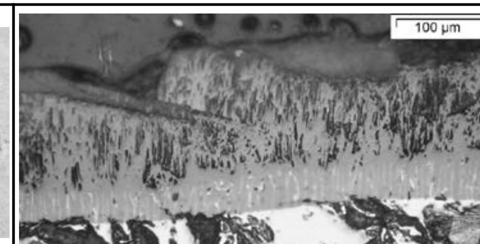
1st rod 940 mm	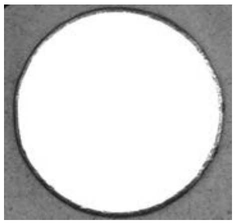	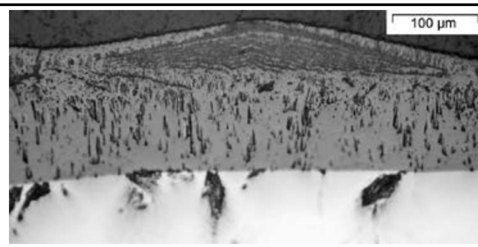	2nd rod 1120 mm	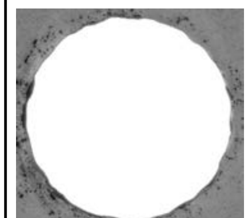	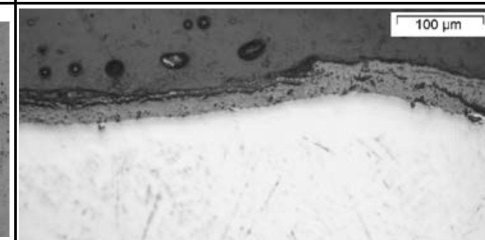
1st rod 1120 mm	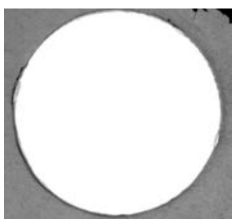	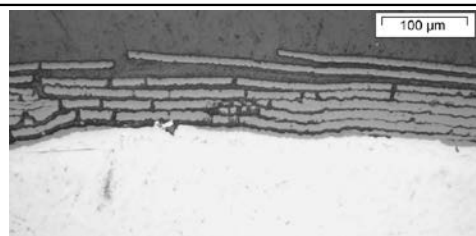	3rd rod 700 mm	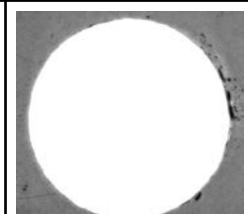	
2nd rod 700 mm	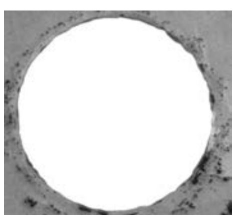	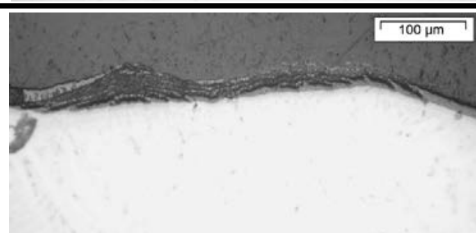	3rd rod 820 mm	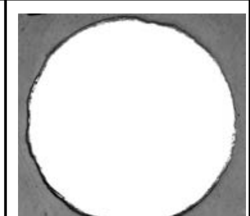	

Breakaway structure was formed generally during pre-oxidation by temperatures about:
850°C (@700 mm), 1100°C (@940 mm), 900°C (@1120 mm)

QUENCH-12: post-test videoscope observations of breakaway oxidation at different elevations of the bundle

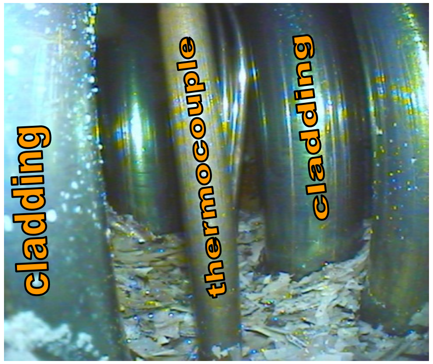

-400mm:
spalled oxide scales
as debris
at the bundle bottom

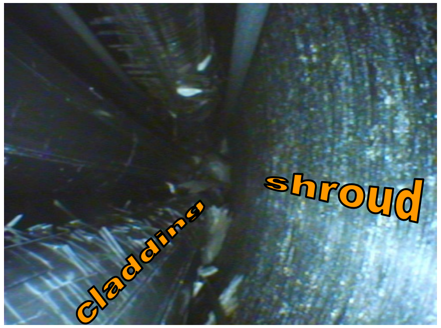

400 mm:
circumferential spalling
of the oxide layer
on the surface
of fuel rod simulator cladding

650 mm:
spalled oxide scales
at shroud and cladding

900 mm:
circumferential
and longitudinal cracks
at the cladding;
nodular breakaway
corrosion at the shroud

QUENCH-12: axial distribution of oxide layer

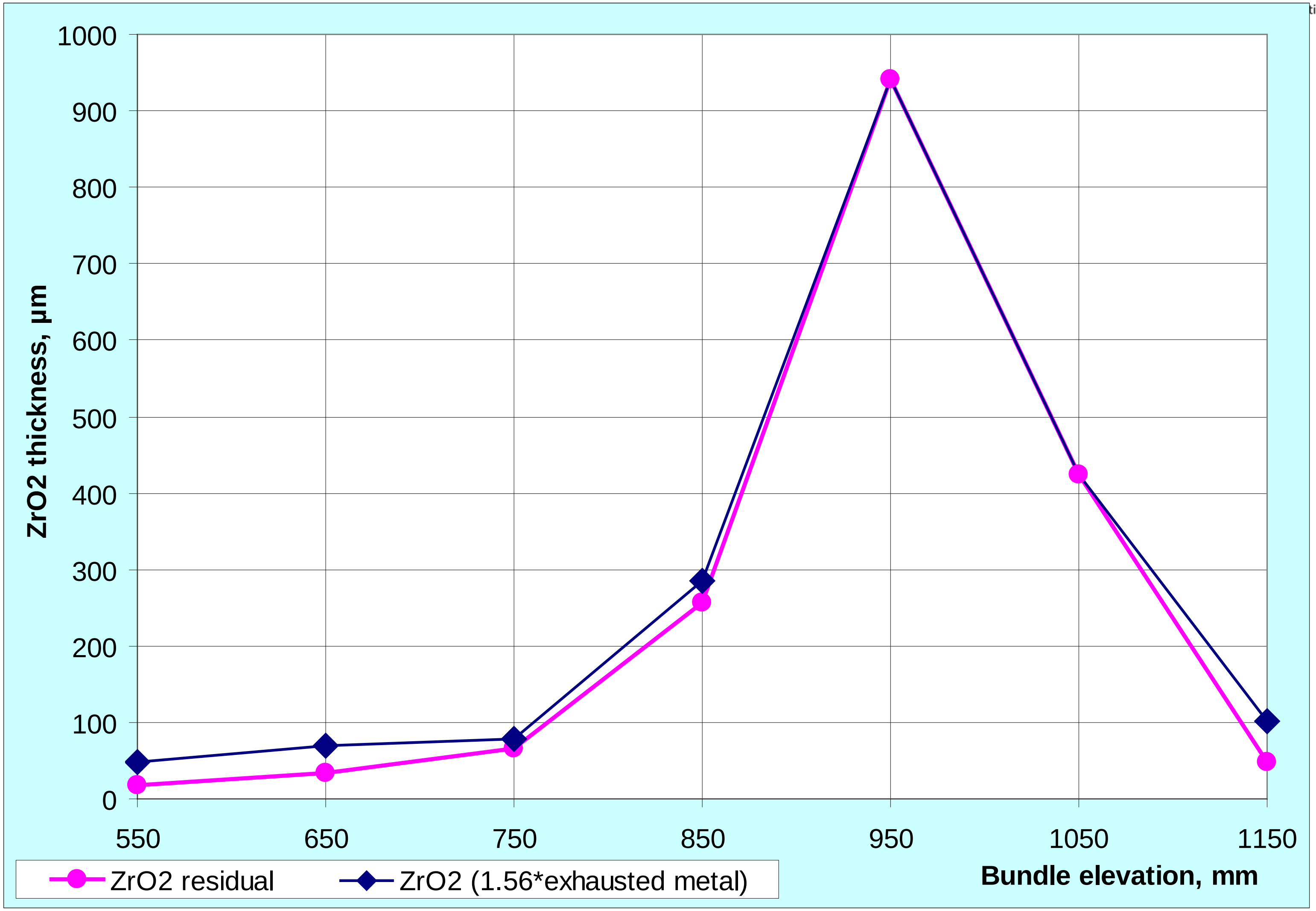

Cladding oxidation: measured thickness of residual oxide and oxide thickness calculated on the base of residual metal

Comparison of oxide cladding thicknesses for QUENCH-06 and QUENCH-12 at elevation 550 mm

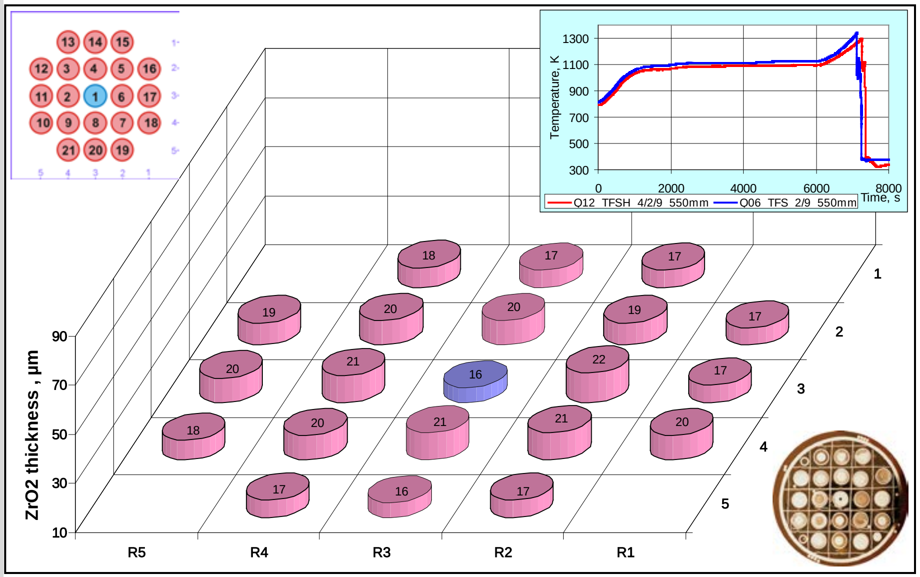

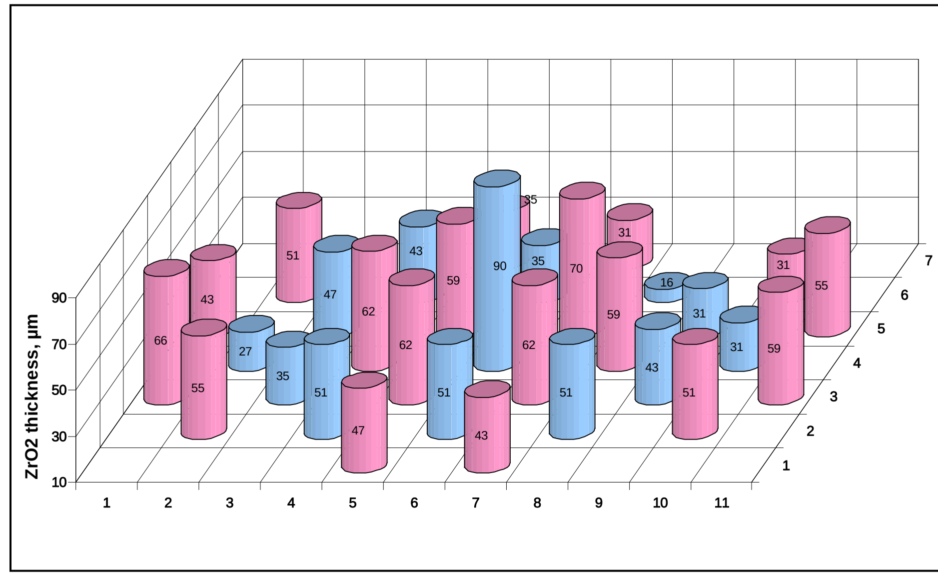

QUENCH-06:
average value and median deviation:
19 ± 2 µm for all rods,
21 ± 1 µm for inner heated rods,
18 ± 1 µm for outer heated rods

QUENCH-12:
average value and median deviation:
42 ± 12 µm for unheated rods,
52 ± 10 µm for heated rods

Comparison cross-sections of QUENCH-06 and QUENCH-12 at elevation 550 mm

Institute of Technology

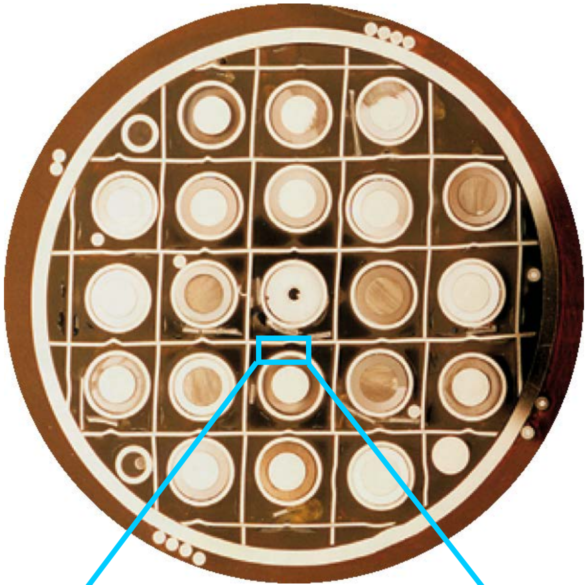

Q06 cross-section

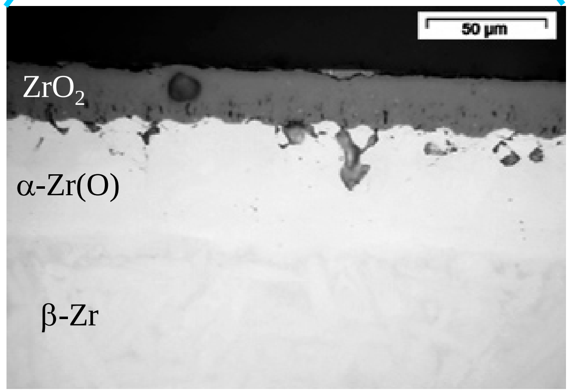

Q06 oxidized cladding

Q12: rubble on spacer grid consists of spalled cladding scales and fragments of partially oxidized cladding

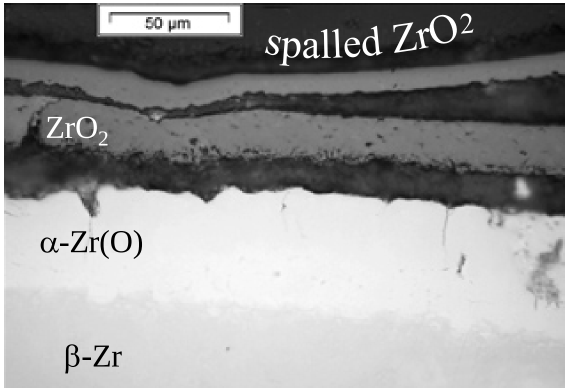

Q12 cladding: spalling of oxide scales due to breakaway effect

Comparison of oxide cladding thicknesses for QUENCH-06 and QUENCH-12 at elevation 750 mm

Karlsruhe Institute of Technology

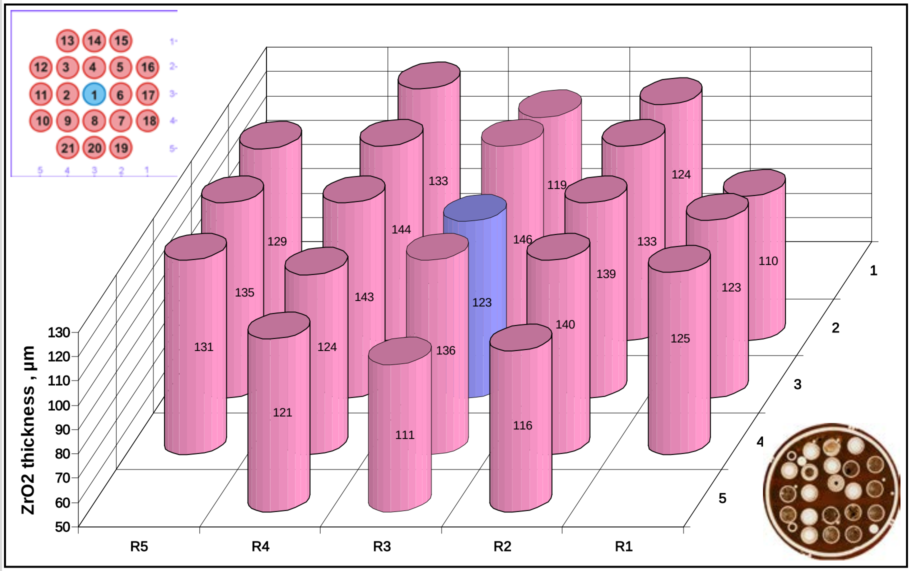

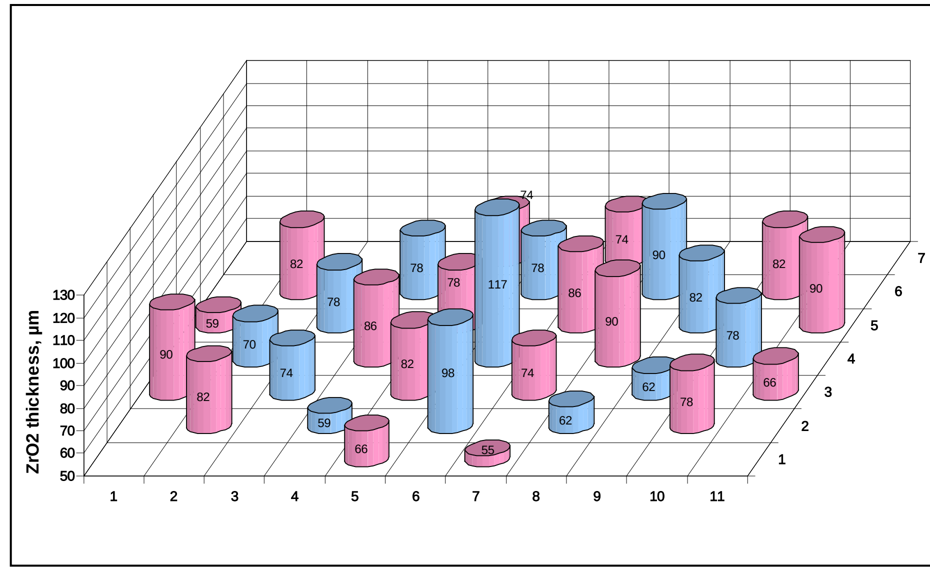

QUENCH-06:
average value and median deviation:
129 ± 9 µm for all rods,
138 ± 5 µm for inner heated rods,
123 ± 6 µm for outer heated rods

QUENCH-12:
average value and median deviation:
79 ± 11 µm for unheated rods,
77 ± 8 µm for heated rods

Comparison cross-sections of QUENCH-06 and QUENCH-12 at elevation 750 mm

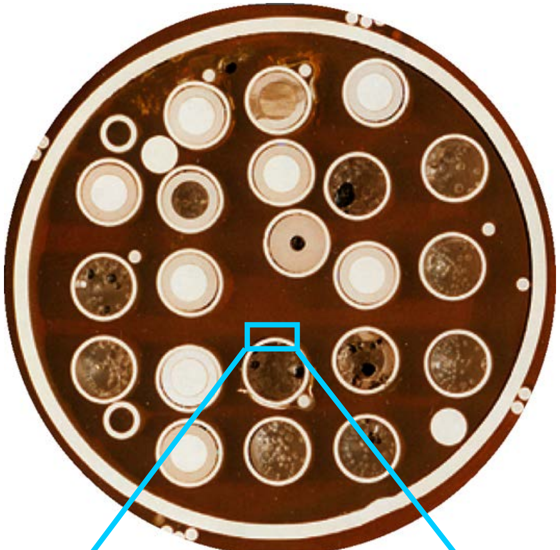

Q06 cross-section; few bundle deformation

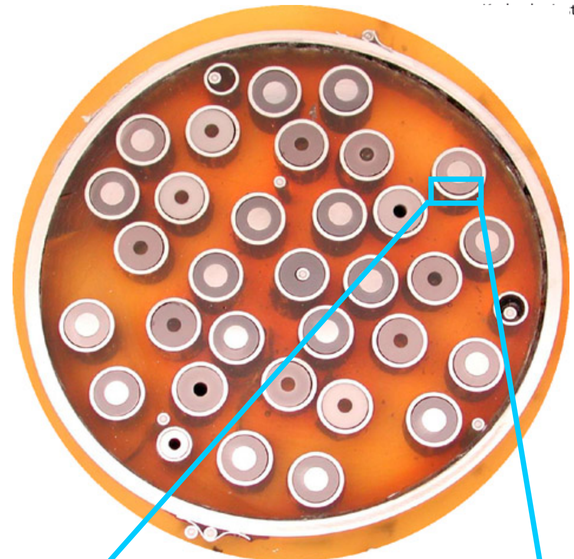

Q12 cross-section; moderate bundle deformation

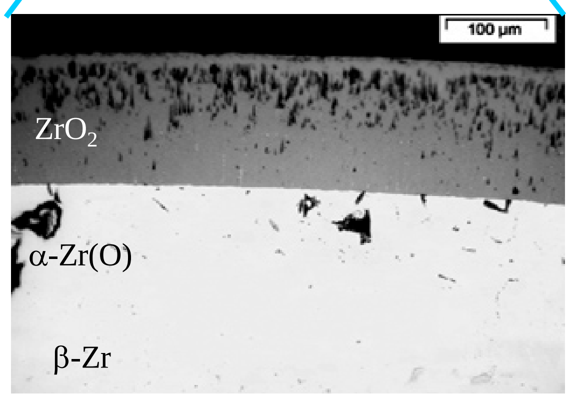

Q06 oxidized cladding

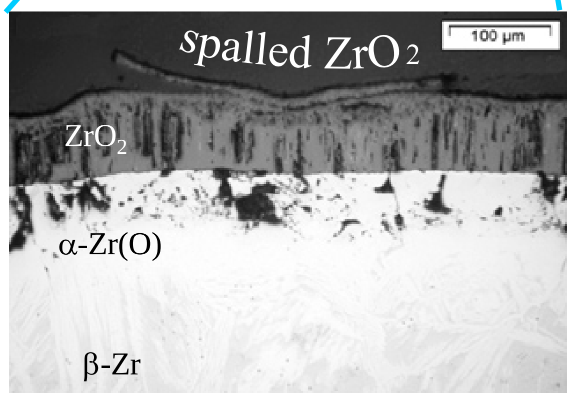

Q12 cladding: spalling of oxide scales due to breakaway effect

Comparison of oxide cladding thicknesses for QUENCH-06 and QUENCH-12 at elevation 1150 mm

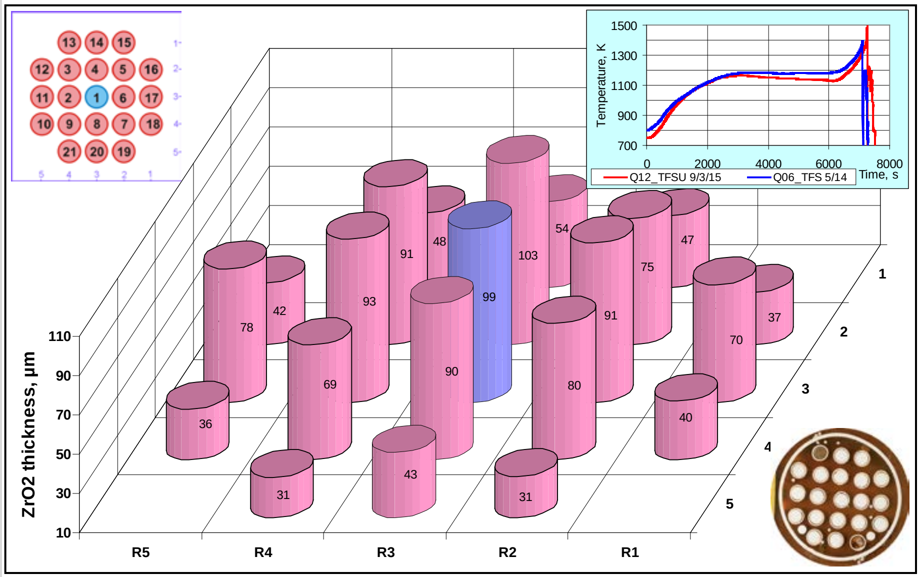

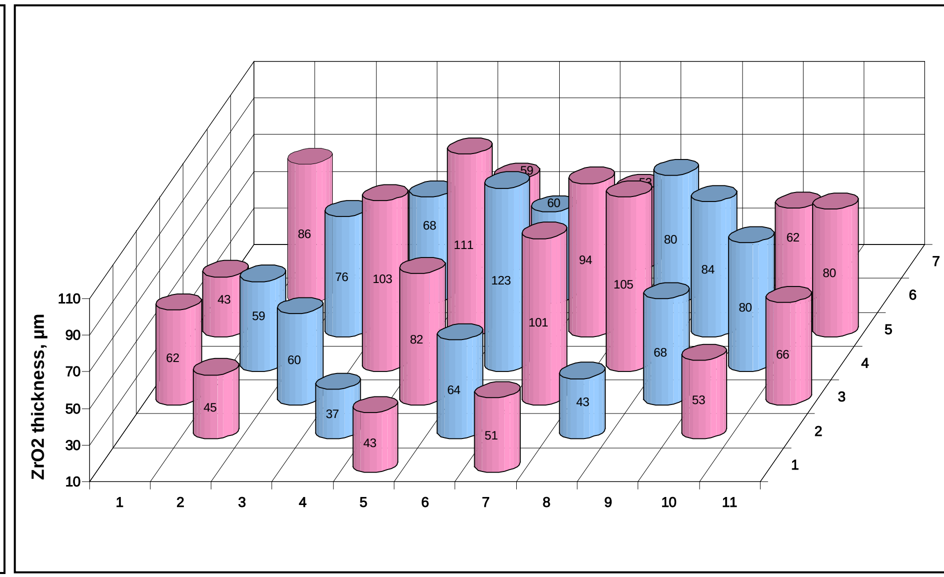

QUENCH-06:
average value and median deviation:
64 ± 22 µm for all rods,
86 ± 9 µm for inner heated rods,
46 ± 11 µm for outer heated rods

QUENCH-12:
average value and median deviation:
69 ± 15 µm for unheated rods,
72 ± 21 µm for heated rods

Comparison cross-sections of QUENCH-06 and QUENCH-12 at elevation 1150 mm

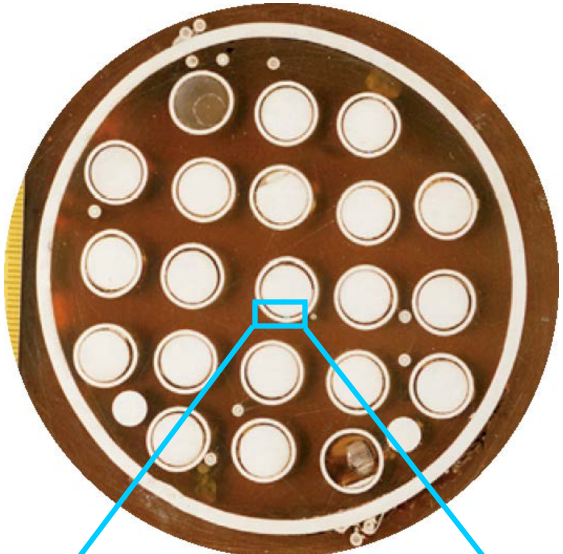

Q06 cross-section

Q12 cross-section

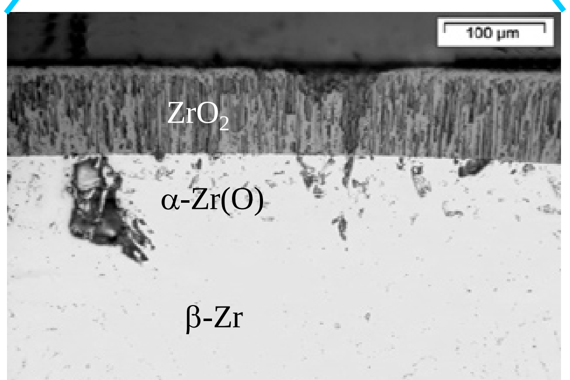

Q06 oxidized cladding

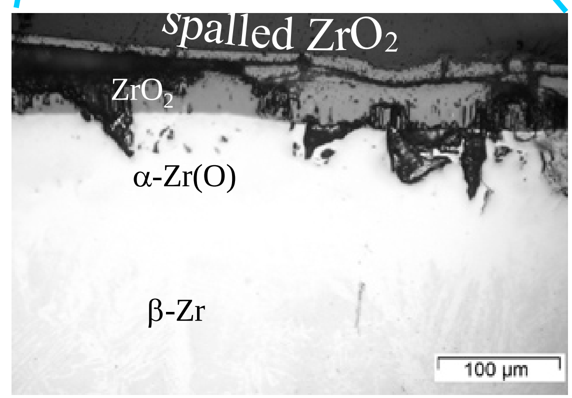

Q12 cladding: spalling of oxide scales due to breakaway effect

Breakaway long-term oxidation during the Paks cleaning tank incident (destroying of 30 VVER fuel assemblies)

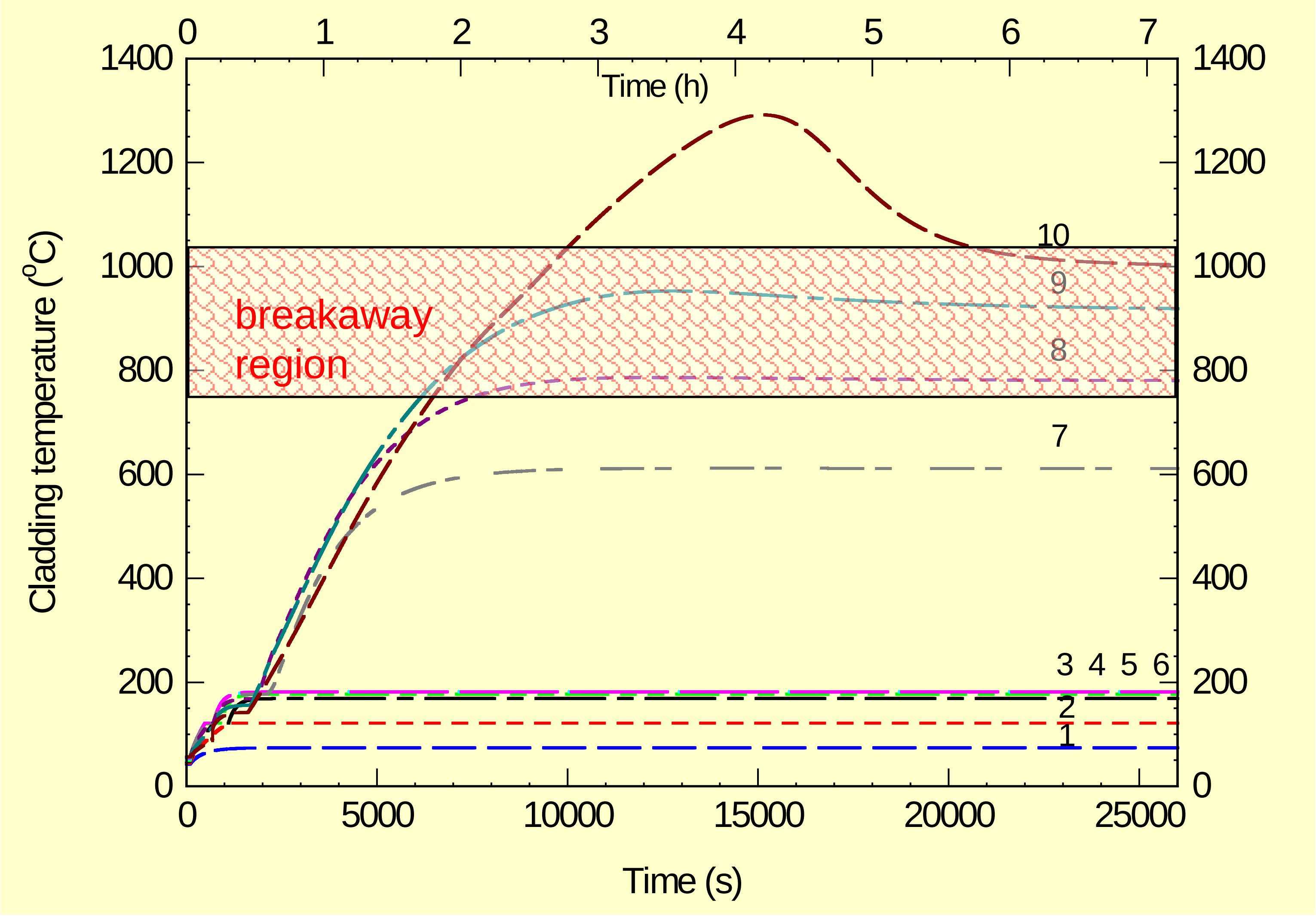

Results of modeling (FRAP-T6 code)

Melt formation for QUENCH-06 and QUENCH-12 at elevation 950 mm

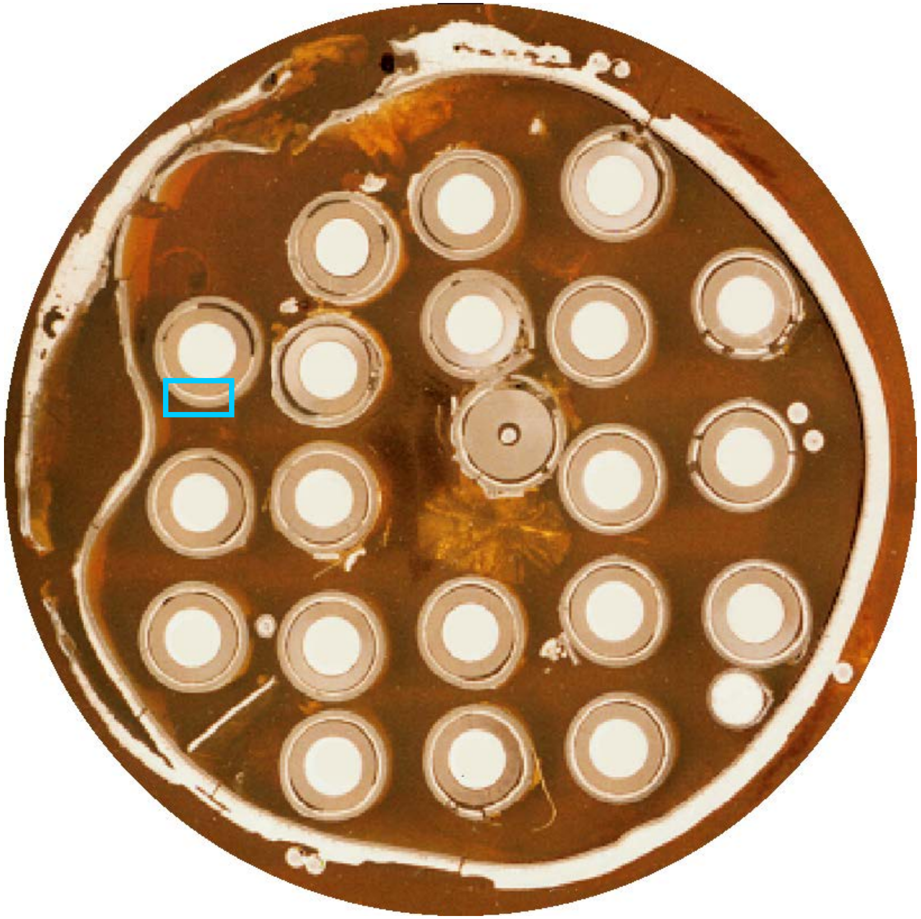

Q06: melting of cladding internal metal layer and shroud external metal layer

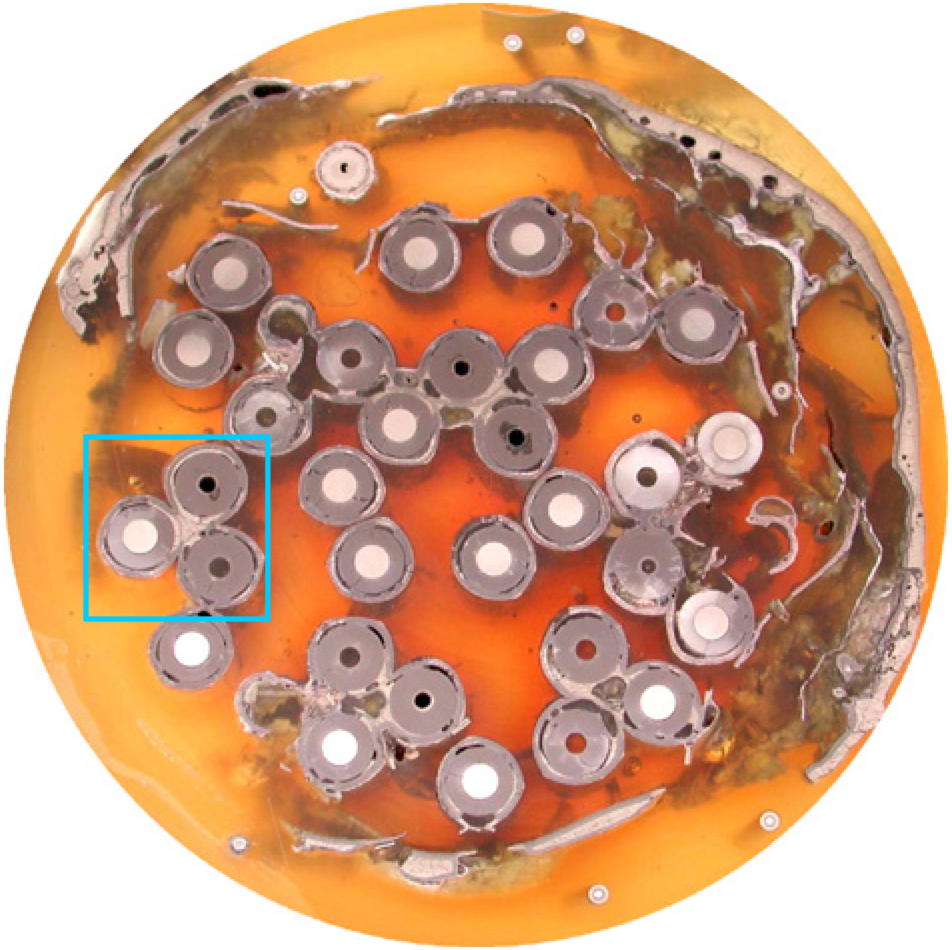

Q12: melting of cladding internal player; oxide layer failure; molten pools formation between rods; shroud external metal layer melting

Melt formation for QUENCH-06 and QUENCH-12 at elevation 950 mm

Karlsruhe Institute of Technology

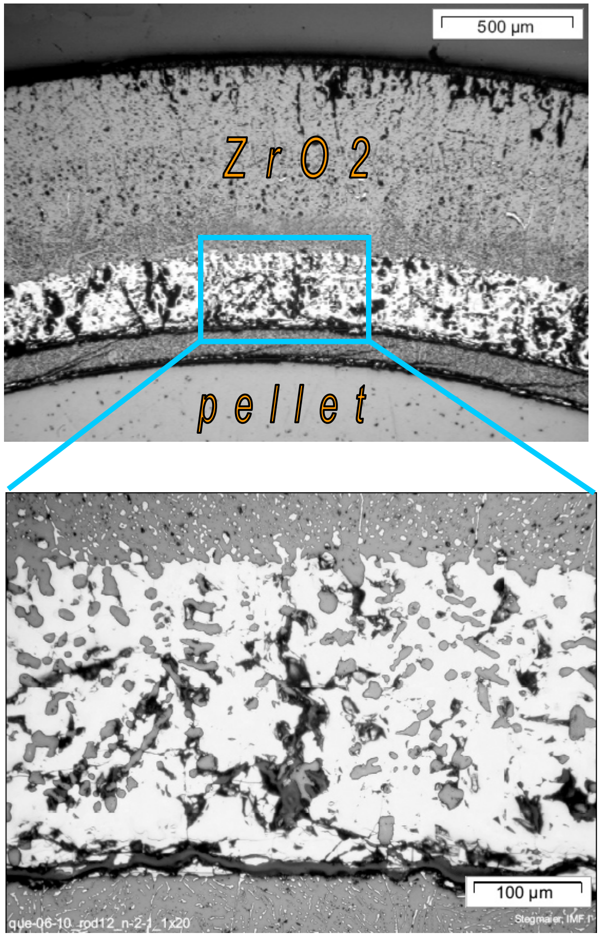

Q06: melting of cladding metal layer

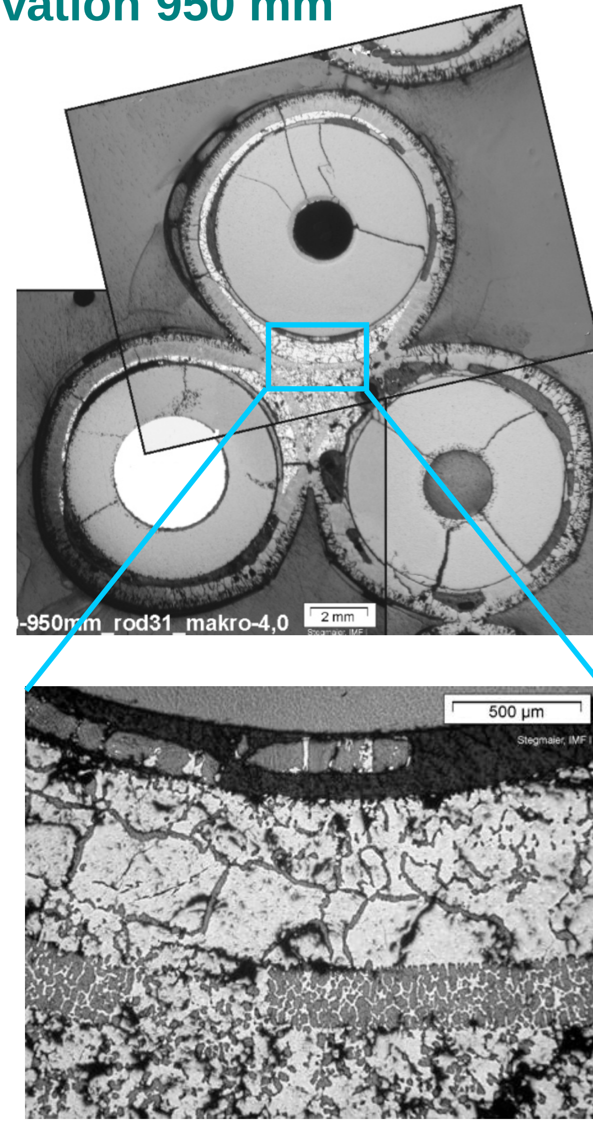

Q12: molten pool between rods

QUENCH-12: results of the SVECHA simulation (IBRAE with support from ITU)

In the SVECHA/QUENCH code the thermal boundary conditions for the central rod are predetermined by specifying the temperatures of the "effective channel" inner wall on the basis of experimentally measured temperatures. The inner surface of the effective channel represents the surfaces of the heated rods surrounding the central rod.

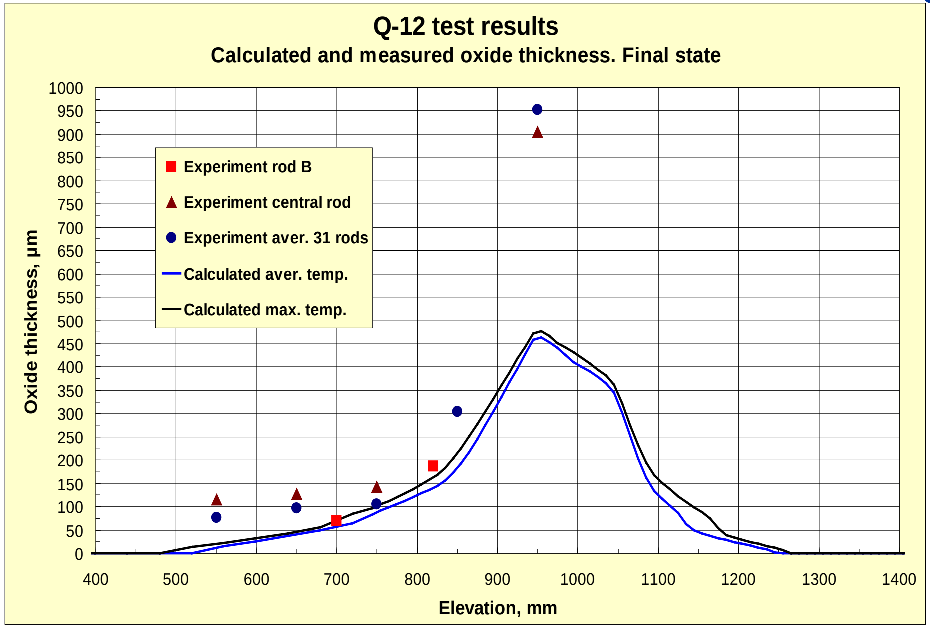

Measured oxide layer thickness profiles of the rod B (withdrawn from the bundle at the end of the test), central rod, averaged for 31 rods, all at final state, compared to the calculated oxide layer thickness profile of the central rod (final state).

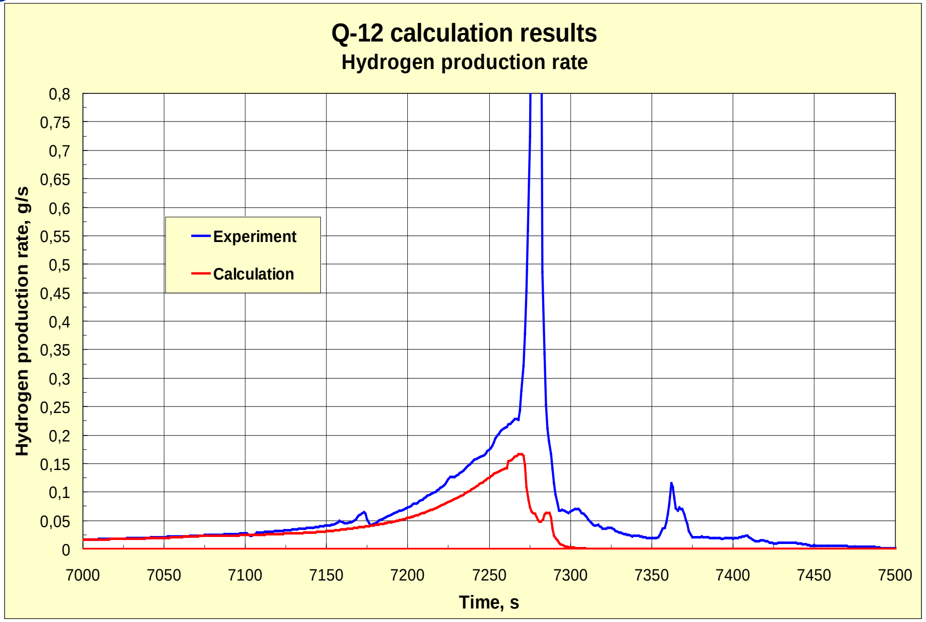

Experimentally measured and calculated hydrogen production rate.

Quenching phase of the test.

Amount of hydrogen released during quenching: 24 g (exp); 9.9 g (calc.)

SUMMARY

- The QUENCH-12 experiment investigated the effects of VVER materials and bundle geometry on core reflood, in comparison with test QUENCH-06 (ISP-45) with Western PWR geometry.

- The electrical power changing during the test corresponds completely to calculated values up to reflood phase. The temperatures at all bundle elevations during preoxidation are about 30 - 40 K lower than during corresponding phase of QUENCH-06.

- Two corner rods were withdrawn at the end of preoxidation and transient phases correspondingly. The third corner rod was withdrawn after the test. The surface of the rods shows intensive traces of the break-away effect influence. Many oxide scales with thickness about 100 µm were spalled during withdrawn.

- The surfaces of the E-110 rod simulator and E-125 shroud evident also influence of the breakaway oxidation. However the ZrO_2 scales spalling is fewer intensive than by corner rods. Possible reasons can be 1) different mechanical properties of tube and massive rod; 2) other surface preparation of cladding and rods.

SUMMARY (cont.)

Karlsruhe Institute of Technology

- Following reflood initiation, a moderate temperature excursion of ca. 50 K was observed, over a longer period than in QUENCH-06. The temperatures at elevations between 850 mm and 1050 mm exceeded the melting temperature of β-Zr.

- Post-test bundle examinations performed at RIAR and KIT showed significantly more oxidised cladding surfaces in comparison to QUENCH-06. Also the radial oxidation inhomogeneity is much higher for QUENCH-12 bundle.

- The hydrogen content in the corner rods reached a value more than 30 at% at the bundle elevations of 850 and 1100 mm.

- The total hydrogen production was 58 g (for QUENCH-06: 36 g), during the reflood was released 24 g hydrogen (for QUENCH-06: 4 g). This may be attributed partly to the longer excursion time in QUENCH-12. Other reasons for the increased hydrogen production may be extensive damaging of the cladding surfaces due to the breakaway oxidation and local melt formation with subsequent melt oxidation.

SUMMARY (modelling)

- The SVECHA/QUENCH code (IBRAE) was applied to the simulation of the QUENCH-12 bundle test. The calculations adequately reproduce temperature evolution of the central rod at different elevations during the whole test duration including quenching phase.

- The calculated oxide thickness at the end of the test was significantly underestimated, especially at 950 mm. This fact may be explained by more intensive oxidation during transient and quenching phases through friable cracked oxide structure formed due to break-away oxidation previously.

- The details of the experimentally measured time dependence of the hydrogen production rate are well reproduced by the calculations at the preoxidation and transient phases. Calculations underestimate hydrogen production rate at the end of transient and quenching phase of the test.

Thank you for your attention

http://www.iam.kit.edu/wpt/english/471.php/

http://quench.forschung.kit.edu/